International Journal of Mechanical, Industrial and Aerospace Sciences
ISSN: 2517-9950
Vol:10, No:5, 2016

Numerical Study on the Hazards of Gravitational Forces on Cerebral Aneurysms

Hashem M. Alargha, Mohammad O. Hamdan, Waseem H. Aziz

***Abstract*—**Aerobatic and military pilots are subjected to high gravitational forces that could cause blackout, physical injuries or death. A CFD simulation using fluid-solid interactions scheme has been conducted to investigate the gravitational effects and hazards inside cerebral aneurysms. Medical data have been used to derive the size and geometry of a simple aneurysm on a T-shaped bifurcation. The results show that gravitational force has no effect on maximum Wall Shear Stress (WSS); hence, it will not cause aneurysm initiation/formation. However, gravitational force cause causes hypertension which could contribute to aneurysm rupture.

***Keywords*—**Aneurysm, CFD, wall shear stress, gravity, fluid dynamics, bifurcation artery.

I. Introduction

AN intracranial aneurysm is a vascular disorder characterized by abnormal focal dilation of a brain artery which is considered as a serious and potentially life-threatening condition. The weariness of the inner muscular layer of a blood vessel wall can cause the abnormal focal dilation of the artery which can compress surrounding nerves and brain tissue resulting in many serious medical conditions. Recently more cases of patients with unruptured intracranial aneurysms are diagnosed due to continuous development of accurate noninvasive cerebrovascular imaging techniques. It has been reported in a clinical study [1] that the occurrence of unruptured intracranial aneurysms is around 6.5% for a sample of 400 adult volunteers (age 39 to 71 years old with mean age of 55 years). The rupture of a cerebral aneurysm usually results in internal bleeding such as a subarachnoid hemorrhage and intracranial hematoma [2]. The importance of studying aneurysms is that it affects around 2% of adults and in case of rupture such condition can lead to death if urgent medical intervention did not take place [3].

It has been shown in literature [4] that, due to gravity force acceleration, the aneurysm position affects the hydrodynamics of brain aneurysms. These results reported [4] that an aneurysm oriented in opposite direction of gravity acceleration, has a very low risk of thrombosis. Also it is reported [4], the greatest flow turbulence against the wall is found in the aneurysm oriented downwards, that is parallel to the force of gravity which causes higher risk of growth and rupture, in comparison with other conditions.

A report by the U.S. Federal Aviation Administration (FAA) mentions that little is known about the effects of high negative gravities on humans and that blood vessels in the brain can only tolerate weak gravitational forces. Four case reports of aircraft accidents due to gravity induced loss of consciousness were presented to proof that intense gravity is very hazardous [5].

It was reported in many cases that aneurysms could rupture due to negative gravitational forces that are induced in roller coaster rides. A case report published by the journal of neurosurgery presents a case of a 32-year old women that developed a traumatic distal anterior cerebral artery aneurysm from a roller coaster ride [6]. The report mentions that a relatively minor trauma caused by a roller coaster ride led to aneurysm formation while severe injuries from falls and road accidents cause aneurysm formation [6].

The aim of this study is to numerically study the effect of high vertical accelerations on hemodynamics and such accelerations can affect the initiation, growth and rupture of cerebral aneurysms. The study reports the effect of vertical acceleration on the WSS, the wall strain and the wall stresses of cerebral aneurysm. Procedure for Paper Submission

II. Problem Formulation

A. Geometric Formulation

A diagram of the computation domain of the terminal aneurysm is modeled using an idealized outline and is shown in Fig. 1 (a). Repetitive impingement against the vessel wall under pulsatile flows may induce fatigue, initiation and growth of aneurysms and it is expected that flow impingement on the tip of terminals generates unstable helical flow patterns near the wall. For the geometry, the model is divided into three sections of interest; (i) the aneurysm, (ii) the parent artery and (iii) the sister arteries. In our model, we are supposing the reasonability of using an idealized geometry. Dimensions for the model are derived from the actual patient angiograph images shown in Fig. 1 (b) in addition to other clinical reports from literature [7]-[9].

The parent artery and the sister arteries are modeled as a tube of diameter $D_{p.a.} = 2.5$ mm and length of $l = 10$ mm. The sister arteries are bifurcating from the parent artery and are given the same radius as the parent artery for simplicity and since such arteries conditions have been observed in clinical patient angiograph image of a patient (Fig. 1 (b)). The length of parent and sister arteries are selected to be $l = 10$ mm. Five cases were studied for aneurysms with $D_a = 0$, 4, 6, and 12, and 12 millimeters for fixed parent arteries $D_{p.a.}$. For the five cases studied the aspect ratio $D_a/D_{p.a.}$ is calculated.

Hashem M. Alargha (Eng.) and Mohammad O. Hamdan (Dr.) are with the United Arab Emirates University, Mechanical Engineering Department, United Arab Emirates (e-mail: mohammadh@uaeu.ac.ae).

Waseem H. Aziz (Dr.) is with the Tawam Hospital, Neuro Endovascular Centre, Al Ain, United Arab Emirates (e-mail: Waseem.aziz@tawam.ae).

Following the work of Sherif et. al. [7], the wall thickness of the aneurysm is modeled to be uniform with $t_a = 0.25$ mm and arteries (parent and sister) of $t_c = 0.46$ mm. The aneurysm wall thickness is less than that the artery due to wall stretching that increases the surface area while the wall thickness shrinks from 0.46 mm to 0.25 mm.

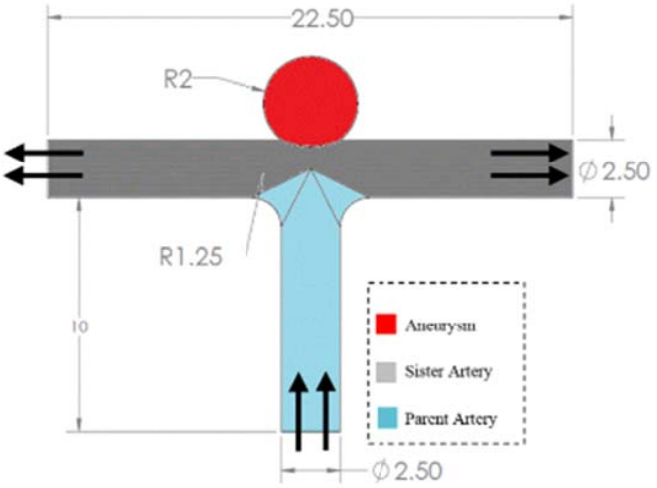

(a)

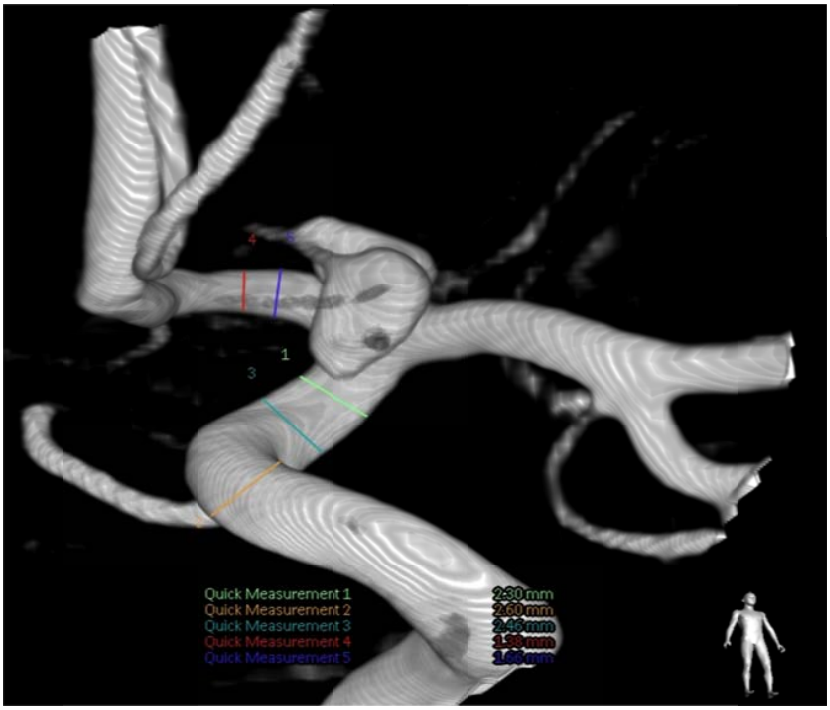

(b)

Fig. 1 Terminal aneurysm geometry (a) schematic diagram used in the FSI analysis, (b) Angiograph image

B. Material Properties

For the blood, the density is taken as 1050 kg/m^3, and based on a previous study by our team, the Newtonian viscosity model assumption is invalid in aneurysmal studies [10]. Hence, the viscosity model considered in this study is the non-Newtonian based on Carreau model with constants proposed by Siebert et al. [11]. For the artery and aneurysm wall, the density, Poisson's ratio and elastic modulus are set to 1120 kg/m^3, 0.4 and 0.9 MPa, respectively. These values closely correspond to those reported for an aged patient for whom the arterial wall is stiffened with an elasticity less than that of a healthy young person [12]-[14].

C. Boundary Conditions

For the blood flow, a steady-state uniform velocity is used at the inlet of the artery with a maximum blood velocity of 0.5 m/s. The maximum blood velocity is used since at this condition maximum pressure is produced which should significantly affect the wall stresses and deformation.

The effect of gravity forces is mainly modeled as blood pressure. Seven gravity settings are investigated in this study from -3g up to 3g including 0g. In all these cases, the outlet static pressures of cerebral aneurysms are calculated as:

$$P_{an} = P_{heart} + \rho\, g\, h$$

where ρ is blood density, g is the gravity acceleration and h is the location of the aneurysm with respect to the heart. The following assumption is used in the calculation:

- This study is estimating that the aneurysm to be 20 cm far away from the heart in the spin direction which represent 10 cm below the head tip.
- The average height of individuals in the UAE is 1.7 meters [15].
- Average blood pressure used in this study 100 mmHg (13332 Pa) and the heart pressure is calculated at 1-g is found to be $P_{heart} = 10.241$ Pa. The average blood pressure is calculated by adding the heart pressure $P_{heart} = 10.241$ Pa to weight of the blood column above the heart (it is estimated the heart is located at 0.3 m below the head tip).

The aneurysms pressure is calculated using the above equation for several g-values (mainly; -3g, -2g, -1g, 0g, 1g, 2g and 3g) and plotted as shown in Fig. 2.

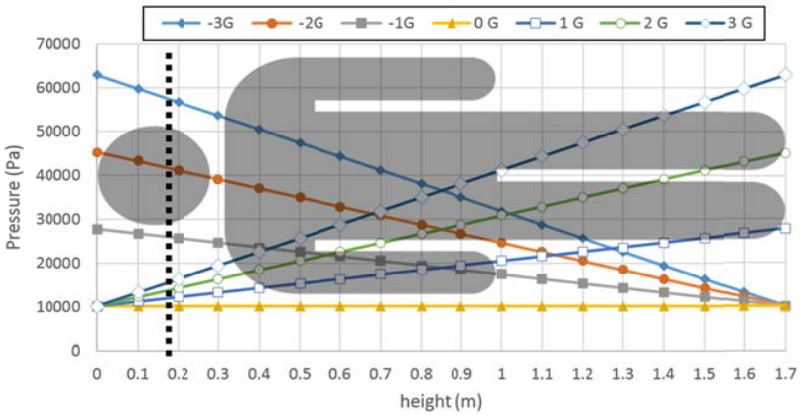

Fig. 2 Pressures along the body for different gravities

D. Numerical Formulation

The model is divided into three sections of interest, the aneurysm dome, the parent artery and the sister arteries. The final mesh used in this study contains around $1.2x10^6$ elements with the minimum mesh size of 0.1 mm. The convergence residuals criteria are set to 1×10^{-6} for all variables. A mesh independence study is implemented to make sure that the output values are independent of mesh size. Fig. 3 shows the maximum WSS at Aneurysm dome vs. Number of grid elements.

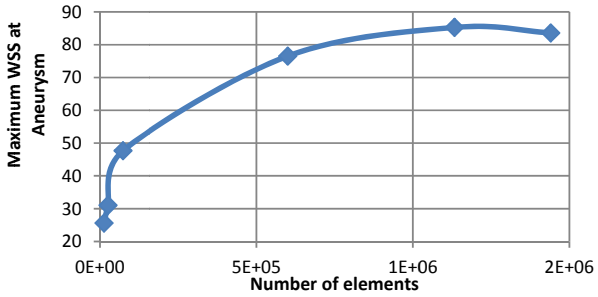

Fig. 3 Maximum WSS versus number of mesh elements

III. Results and Discussion

The effects of g-force acceleration, that is aligned with spinal cord, is investigated in this study and is identified as z-axis acceleration. The study addresses the effect of g-force acceleration value and direction on the hemodynamics, hypertension and blood vessel forces. The study reports how g-force acceleration affects blood pressure inside cerebral aneurysm which consequently affects the WSS, the wall stresses and the wall deformation. The present problem is solved using ANSYS-Fluent.

It has been reported in different places in literature [16], [17] that WSS inside an aneurysms are in the range of 3-8 Pa which is also reported in this study as shown in Fig. 6 (a). Secondly, a sensitivity study has been conducted by our research team to investigate the effect of Newtonian and non-Newtonian viscous models [10]. The study [10] shows high discrepancy (~50%) between both viscous models at high velocity however a small discrepancy (less than 10%) is detected at low velocity. Lastly, as shown in Fig. 3, a mesh independent study has been conducted through numerical experimentations and mesh refinements which has led to the use of 1.2 million elements.

The contours for WSS and wall stresses under 1-g z-axis

acceleration and aneurysm AR are shown on Fig. 4. As shown from on Fig. 4, the maximum WSS occurs at the apex of the bifurcation. It is expected that flow impingement on the apex of the bifurcation causes the maximum WSS near the wall stagnation point which may prompt fatigue and possible initiation of the aneurysms. Also, it is clear that as AR increases the wall stress start shifting from the parent artery to the aneurysm neck.

Fig. 5 shows the contours for WSS, wall stresses and deformation for AR=2.4 and under different z-axis g-force acceleration. As shown from on Fig. 5, the WSS map does not change as acceleration changes. However, wall stresses and wall deformation change with acceleration. As shown in the figure., negative acceleration produces higher wall stress and deformation when compared to positive acceleration while the location of maximum wall stresses and wall deformation stays the same.

The contours for WSS and wall stresses under 1-g z-axis acceleration and aneurysm AR are shown on Fig. 4. As shown from on Fig. 4, the maximum WSS occurs at the apex of the bifurcation. It is expected that flow impingement on the apex of the bifurcation causes maximum WSS near the wall stagnation point which may prompt fatigue and possible initiation of the aneurysms.

Fig. 6 (a) shows how the area averaged WSS changes under z-axis g-force accelerations, and Fig. 6 (b) shows how the area averaged WSS changes under the different aneurysm aspect ratios. It is clear from Fig. 6 (a) that for a fixed AR, the area averaged WSS does not depends on z-axis g-force acceleration which is expected since the g-force acceleration acts as body force that affect the blood pressure however it will not affect the pressure difference across the artery length. The area averaged WSS depends on the pressure difference and not on the pressure value, hence the hemodynamics does not change and accordingly the area averaged WSS does not change.

Cases @ 1G	WSS Contours	Wall Stress Contours
AR = 0	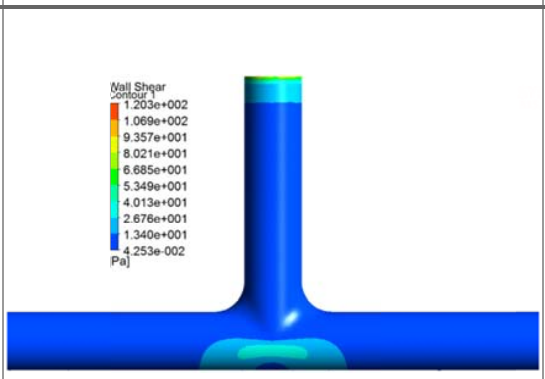	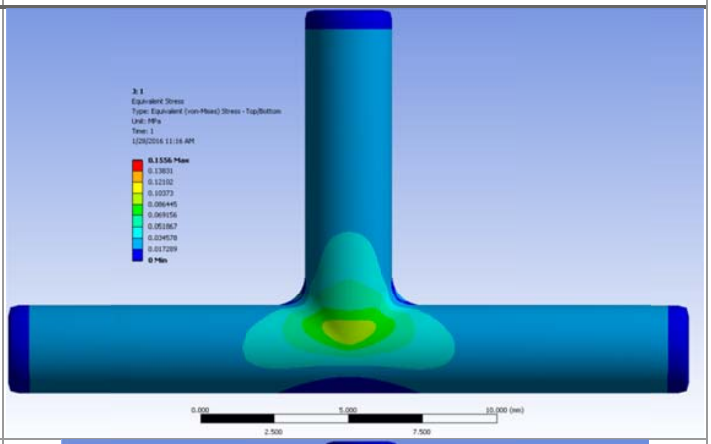
AR = 1.6	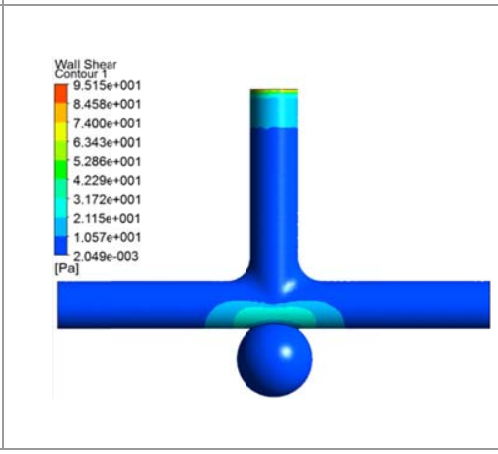	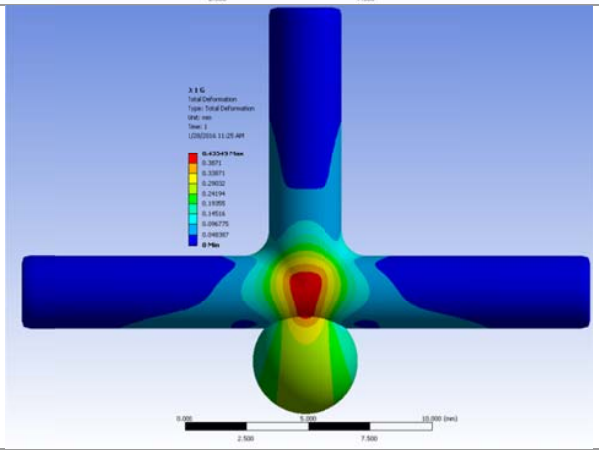

Cases @ 1G	WSS Contours	Wall Stress Contours
AR = 2.4	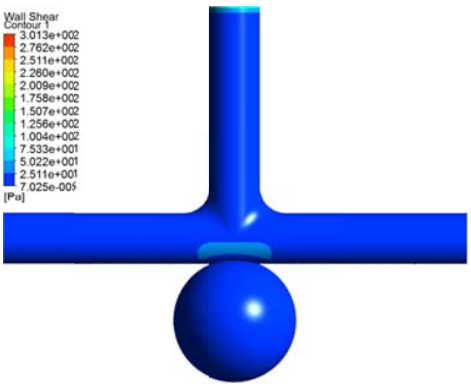	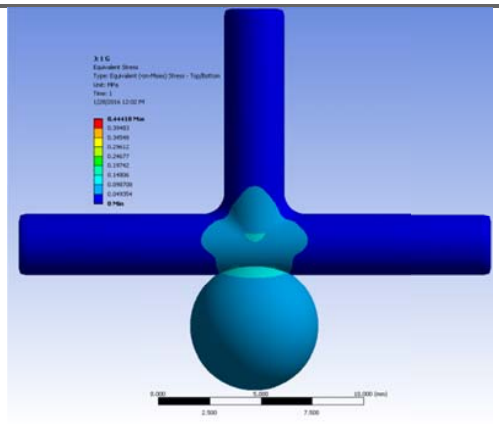
AR = 3.2	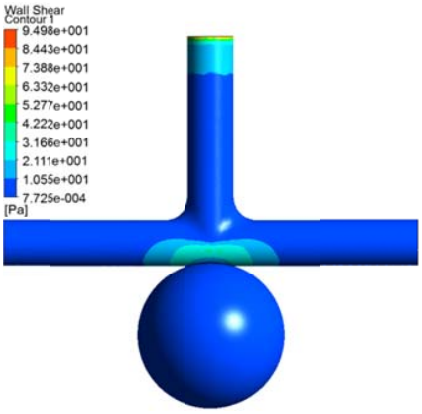	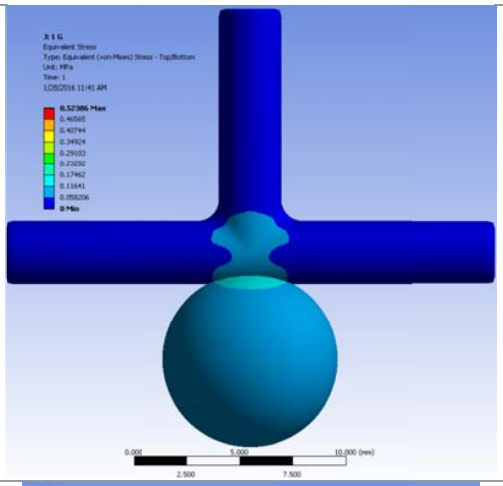
AR = 4.8	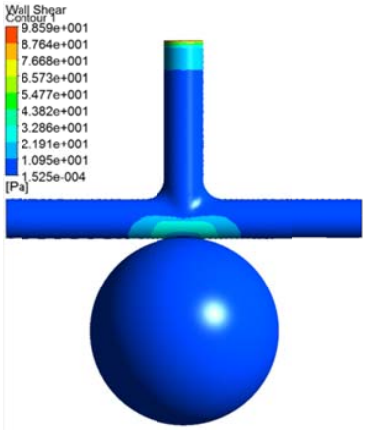	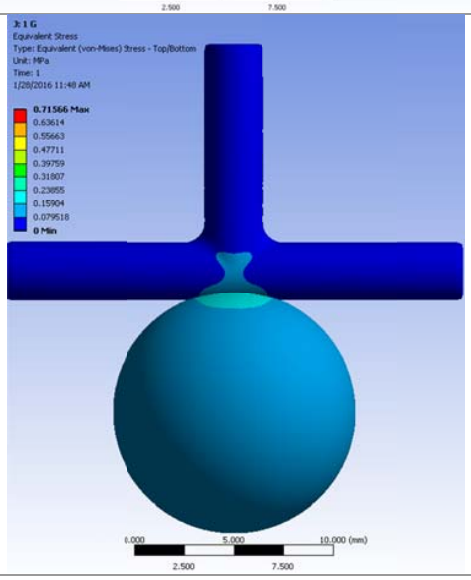

Fig. 4 Contour of WSS and wall stresses are shown for 1-g z-axis acceleration and different values of AR

Fig. 6 (b) shows that the z-axis g-force accelerations did not affect the area averaged WSS as discussed earlier. Also Fig. 6 (b) shows that area averaged WSS decreases as aneurysm aspect ratio increases. This due to the fact that the blood velocity decreases (which affect the rate of flow deformation) as aneurysm size increases which leads to lower area averaged WSS at the aneurysm. The blood velocity decreases inside the aneurysm due to mass conservation in which the blood has

bigger area to pass through which produce weaker blood circulation. As shown in Fig. 6 (b), the WSS is highest for a healthy bifurcation (at zero AR) which could tear the inner wall of the artery possible (with other medical conditions) causing the initiation of the aneurysm.

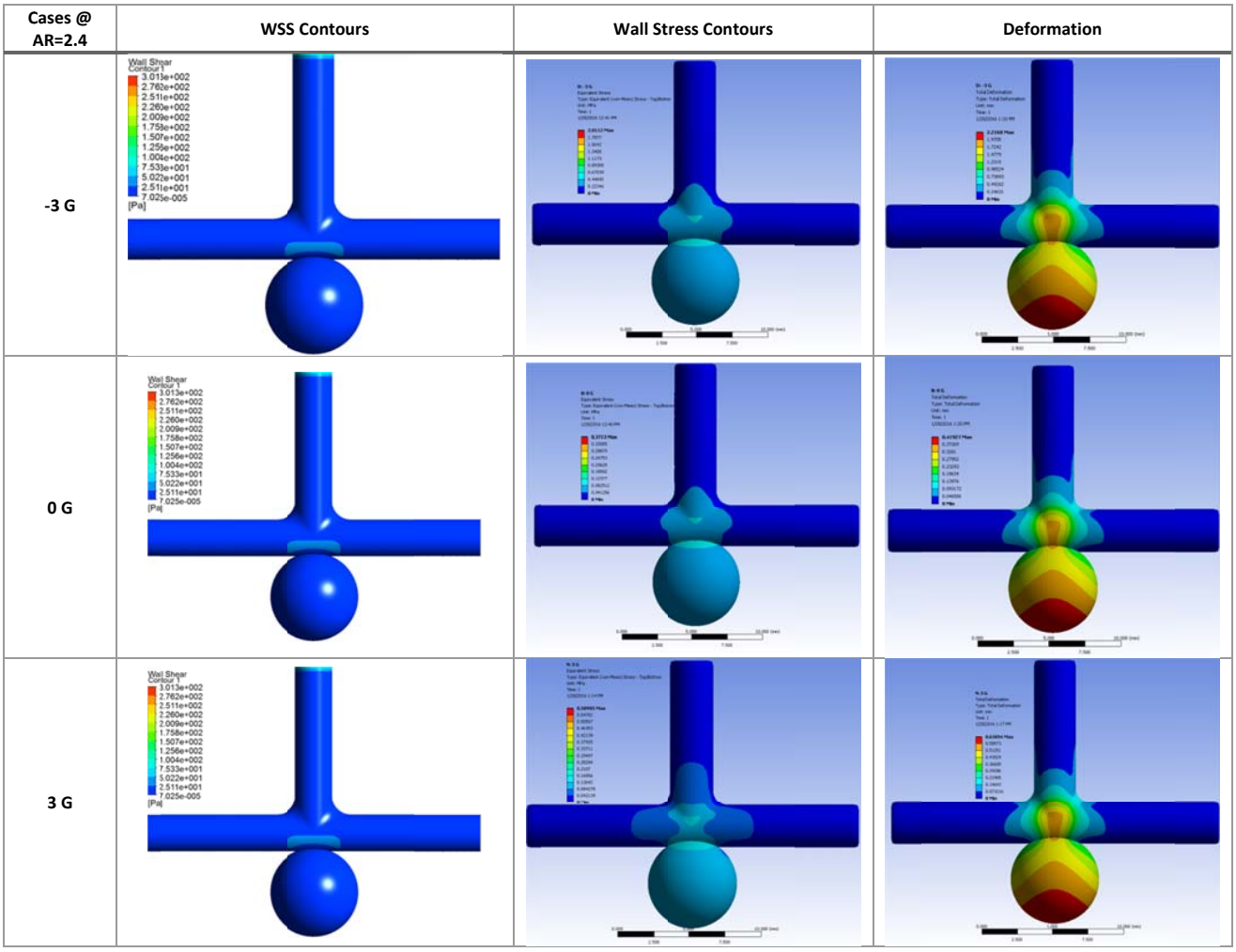

Fig. 5 Contour of WSS, wall stresses and wall strain are shown for AR of 2.4 and for different values of z-axis acceleration

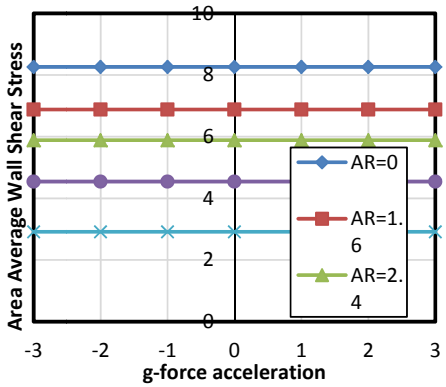

(a)

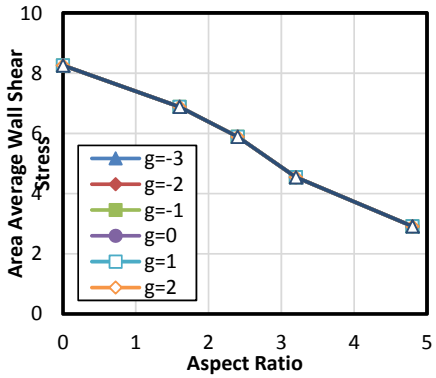

(b)

Fig. 6 The variation of area averaged WSS with respect to (a) g-force acceleration and (b) Aspect ratio

IV. Conclusion

This study uses computational fluid dynamics analysis coupled with finite element analysis methods to explain how hypertension results from z-axis g-force acceleration and how that affects the aneurysm initiation, growth and possible rupture. An idealized aneurysm geometry is used to show that area averaged WSS is independent of z-axis acceleration, which means that such acceleration does not contribute to aneurysm formation/initiation.

Acknowledgment

Authors would like to thank Eng. Youssef Shaaban for Fluent troubleshooting.

References

[1] T. Nakagawa and K. Hashi, "The incidence and treatment of asymptomatic, unruptured cerebral aneurysms," Journal of neurosurgery, vol. 80, pp. 217-223, 1994.
[2] T. Otani, M. Nakamura, T. Fujinaka, M. Hirata, J. Kuroda, K. Shibano, et al., "Computational fluid dynamics of blood flow in coil-embolized aneurysms: effect of packing density on flow stagnation in an idealized geometry," Medical & biological engineering & computing, vol. 51, pp. 901-910, 2013.
[3] G. J. Rinkel, M. Djibuti, A. Algra, and J. Van Gijn, "Prevalence and risk of rupture of intracranial aneurysms a systematic review," Stroke, vol. 29, pp. 251-256, 1998.
[4] I. Madrazo, A. Noyola, C. Piña, A. Graef, M. Olhagaray, S. Gutiérrez, et al., "(Effect of position with respect to gravitational force on the hydrodynamics of an experimental model of saccular aneurysm)," Archivos de investigacion medica, vol. 21, pp. 103-113, 1989.
[5] D. Beaudette, "A hazard in aerobatics: Effects of G-forces on pilots," FAA advisory circular, pp. 91-61, 1984.
[6] M. Senegor, "Traumatic pericallosal aneurysm in a patient with no major trauma: Case report," Journal of neurosurgery, vol. 75, pp. 475-477, 1991.
[7] C. Sherif, G. Kleinpeter, G. Mach, M. Loyoddin, T. Haider, R. Plasenzotti, et al., "Evaluation of cerebral aneurysm wall thickness in experimental aneurysms: Comparison of 3T-MR imaging with direct microscopic measurements," Acta neurochirurgica, vol. 156, pp. 27-34, 2014.
[8] V. Costalat, M. Sanchez, D. Ambard, L. Thines, N. Lonjon, F. Nicoud, et al., "Biomechanical wall properties of human intracranial aneurysms resected following surgical clipping (IRRAs Project)," Journal of biomechanics, vol. 44, pp. 2685-2691, 2011.
[9] Y. Bazilevs, M.-C. Hsu, Y. Zhang, W. Wang, T. Kvamsdal, S. Hentschel, et al., "Computational vascular fluid–structure interaction: methodology and application to cerebral aneurysms," Biomechanics and modeling in mechanobiology, vol. 9, pp. 481-498, 2010.
[10] H. M. AlArgha, M. O. Hamdan, A. Elshawarby, and W. H. Aziz, "CFD Sensitivity study for Newtonian viscosity model in cerebral aneurysms," presented at the Eleventh International Conference on Computational Fluid Dynamics in the Minerals and Process Industries, Melbourne, Australia, 2015.
[11] M. W. Siebert and P. S. Fodor, "Newtonian and non-newtonian blood flow over a backward-facing step–a case study," in Proceedings of the COMSOL Conference, Boston, 2009.
[12] J. D. Humphrey and S. DeLange, An introduction to biomechanics: solids and fluids, analysis and design: Springer Science & Business Media, 2013.
[13] R. G. Gosling and M. M. Budge, "Terminology for describing the elastic behavior of arteries," Hypertension, vol. 41, pp. 1180-1182, 2003.
[14] W. Nichols, M. O'Rourke, and C. Vlachopoulos, McDonald's blood flow in arteries: theoretical, experimental and clinical principles: CRC Press, 2011.
[15] Y. M. Abdulrazzaq, M. A. Moussa, and N. Nagelkerke, "National growth charts for the United Arab Emirates," Journal of epidemiology, vol. 18, pp. 295-303, 2008.
[16] Y. Zhang, W. Chong, and Y. Qian, "Investigation of intracranial aneurysm hemodynamics following flow diverter stent treatment," Medical engineering & physics, vol. 35, pp. 608-615, 2013.
[17] M. Shojima, M. Oshima, K. Takagi, R. Torii, M. Hayakawa, K. Katada, et al., "Magnitude and role of wall shear stress on cerebral aneurysm computational fluid dynamic study of 20 middle cerebral artery aneurysms," Stroke, vol. 35, pp. 2500-2505, 2004.